2021 International Conference on Unmanned Aircraft Systems (ICUAS)
Athens, Greece. June 15-18, 2021

Design of an Aerial Manipulator System Applied to Capture Missions

Wenyu Zhang[1], Qianyuan Liu[1], Meng Wang[1], Jindou Jia[1],
Shangke Lyu[2,*], Kexin Guo[1,2,*], Xiang Yu[1,2], and Lei Guo[1,2]

***Abstract*— This paper proposes the design of an aerial manipulator system for capture missions. A novel mechanical layout is designed. A 5-degree-of freedom manipulator and the battery are placed at the front and back part of a quadrotor unmanned aerial vehicle (UAV) respectively. This layout can expand the task space and minimize the shift of the center of mass. To improve the success rate of capture, inspired by the predation maneuver of birds, online trajectory generation law for capture mission is proposed. The aerial manipulator points towards its target during the flight. Experimental results show that the proposed aerial manipulator system can capture the target on a moving platform successfully.**

I. INTRODUCTION

During the past few decades, quadrotor unmanned aerial vehicle (UAV) has been broadly applied to both military and civilian domains [1]. Besides exploration and surveillance, it is highly desirable to execute "active" missions including grasping and manipulating. This leads to the creation of aerial manipulator which normally consists of a UAV as the base and a multi-link robotic arm as the manipulator.

The development of the aerial manipulator is reviewed in [2-4]. With respect to modeling and control, the existing methods can be divided into the integrated approach and the separated approach. The former considers the overall aerial manipulator system as one controlled object. The later usually designs two separated controllers for the UAV and the manipulator respectively.

By using the Lagrange equation, the dynamic model of the overall aerial manipulator can be found in [5], [6]. One of the difficulties of the integrated approach is that the dynamic model of the whole system is quite complex. Therefore, it is hard to specify the controllers accordingly. In order to simplify the dynamic model, the reference [7] restricts the task space of the aerial manipulator system to a plane. On the other hand, many groups prefer to using the separated approach where the inner dynamic coupling is treated as the disturbance acting on the UAV and the manipulator respectively. Thus it results in a relatively simple model compared to the integrated approach. Along this path, in [8], a torque sensor is used to measure the disturbance acting on the UAV due to the movements of the manipulator. The measured disturbance torque is compensated in the controller of the UAV. The reference [9] analyzes the coupling effect model between the UAV and manipulator.

During the tasks execution, to avoid the rigid contact with the environment, Cartesian impedance control is introduced in [10], [11]. To improve the stability and maneuverability of the aerial manipulator systems, some researchers seek the help from the innovative structures [12], [13]. In [12], a novel mechanism is proposed by utilizing a moving battery to counterweight the statics of the manipulator. To overcome the underactuation problem of UAV, the orientation of thrust force generated by each propeller of the UAV can be different instead of along the same line in [13].

However, there are still some drawbacks in the existing literatures: (1) The degree of freedom (DOF) of the manipulator is low, which limits its task space [7], [9]. With the increase of the DOF of the manipulator, the dynamic model of the aerial manipulator becomes more challenging from both design and control aspects [14-17]. (2) Innovative aerial manipulators always consist of complicated mechanical structure. Thus, it is difficult to design the control law. Moreover, these mechanical structures designed for special purposes may cause other problems such as the lower energy efficiency [12], [13]. (3) Few attention is paid on how to cooperatively plan the path of both the UAV and the manipulator for capture missions [18].

In this paper, an aerial manipulator system is designed and applied to capture a target on a moving platform. As compared to the existing results, the main contributions of this paper are summarized as follows

1) A 5-DOF manipulator is integrated with the quadrotor UAV. A separated control scheme is applied for capture missions.
2) The base link of the manipulator is located at the front part of the quadrotor UAV to expand the task space of the manipulator. By this means, the aerial manipulator can adapt to more complicated missions, e.g., the task that needs the manipulator to penetrate into a hole. On the other hand, this layout can protect the target from the airflow generated by the quadrotor UAV. In addition, the battery is placed on the back part of the

This research was supported by the National Key Research and Development Program of China (Grant number 2020YFA0711200), National Natural Science Foundation of China (Project numbers 61833013, 61903019, 91973012, and 62003018), Program for Changjiang Scholars and Innovative Research Team (Project number IRT 16R03), China Postdoctoral Science Foundation (Grant numbers 2019M660404, 2020M681797, and 2020T130042), Key Research and Development Program of Zhejiang (Grant number 2021C03158), Science and Technology Key Innovative Project of Hangzhou (Grant number 20182014B06), Zhejiang Provincial Natural Science Foundation (Grant number LQ20F030006), and Defense Industrial Technology Development Program (Grant number JCKY2020601C016).

[1] School of Automation Science and Electrical Engineering, Beihang University, 100191, Beijing, China.

[2] Hangzhou Innovation Institute, Beihang University, 310051, Hangzhou, China.

* Corresponding authors.

E-mail: {wyzhang, liuqianyuan, mwbuaa001, lvshangke, kxguo, xiangyu_buaa, lguo}@buaa.edu.cn.

2021 International Conference on Unmanned Aircraft Systems (ICUAS) | 978-1-6654-1535-4/21/$31.00 ©2021 IEEE | DOI: 10.1109/ICUAS51884.2021.9476743

TABLE I: Nomenclature

Symbols	Physical interpretations
m_m	the mass of the manipulator
m_b	the mass of the battery
m_s	the total mass of the aerial manipulator
$\boldsymbol{I}$	the inertia matrix of the quadrotor UAV in B
$\boldsymbol{p} = [x, y, z]^\top$	the position of the quadrotor UAV
$\boldsymbol{v} = [\dot{x}, \dot{y}, \dot{z}]^\top$	the velocity of the quadrotor UAV
$\boldsymbol{a} = \dot{v}$	the acceleration of the quadrotor UAV
$\boldsymbol{\eta} = [\phi, \theta, \psi]^\top$	the Euler angles
$\boldsymbol{\omega} = [p, q, r]^\top$	the angular velocity of the quadrotor UAV
$g = 9.8m/s^2$	the gravitational acceleration
d_ϕ	the half of roll motor-to-motor distance
d_θ	the half of pitch motor-to-motor distance
$[\tau_x, \tau_y, \tau_z]^\top$	the torque of the quadrotor UAV in B
f	the total lift force of the quadrotor UAV along z axis of B
$f_i, \quad i = 1, 2, 3, 4$	the lift force of i_{th} propeller
c_τ	the fixed constant reflecting the relationship between f_i and τ_z

quadrotor UAV to compensate the shift of center of the mass (COM) caused by the manipulator partially.

3) Inspired by the predation maneuver of birds, an online trajectory generation law is designed. The aerial manipulator can generate its trajectory in real time according to the position of the target and complete the capture mission. In the experiment, the aerial manipulator points towards its target at all times to improve the success rate of capture.

The reminder of the paper is organized as follows. Section II analyses the design and architecture of the aerial manipulator. Section III describes the implementation of trajectory generation and control. In Section IV, the flight test results are presented and analyzed. Section V concludes this paper.

Notation 1: Throughout this paper, s_*, c_*, and t_* denote $\sin(*)$, $\cos(*)$, and $\tan(*)$, respectively. For a matrix $\boldsymbol{A}$, notation $\boldsymbol{A}^\top$ denotes its transpose. For a vector $\boldsymbol{x}$, notation $||\boldsymbol{x}||$ denotes its Euclidean norm which is defined as $||\boldsymbol{x}|| = \sqrt{(\boldsymbol{x}^\top \boldsymbol{x})}$. $\boldsymbol{x}^E$ represent that the vector $\boldsymbol{x}$ is represented in E frame. For convenience, the symbols used in this paper are summarized in Table. I.

II. DESIGN AND ARCHITECTURE OF THE AERIAL MANIPULATOR SYSTEM

A. Mechanical Layout

As shown in Fig. 1 (a), in traditional layout of the aerial manipulator, the battery and the manipulator are connected

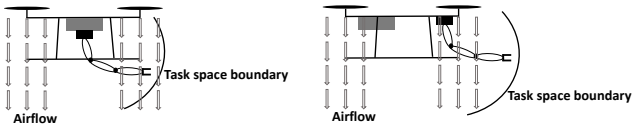

a. Traditional layout b. Proposed layout

Fig. 1: Layout of aerial manipulator.

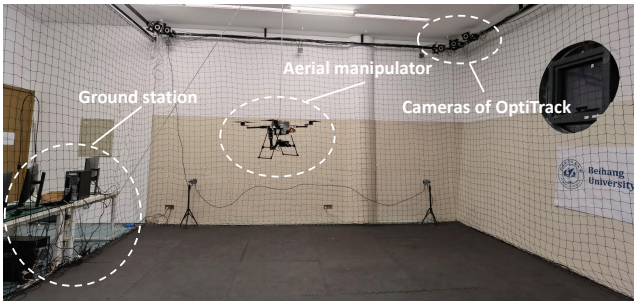

Fig. 2: BUAA aerial manipulator system.

at the COM of the quadrotor UAV to avoid the shift of the COM of overall system. As a result, the task space of the manipulator is located below the quadrotor UAV, which limits the applications of the manipulator. Moreover, the airflow generated by the propeller has an adverse impact on capture missions.

In this paper, a novel layout is proposed as shown in Fig. 1 (b). The base link of the manipulator is located at the front part of the quadrotor UAV. The battery (the gray square in Fig. 1) is placed at the back part of the quadrotor UAV to compensate the shift of COM caused by the manipulator partially. With this mechanical layout, the task space of the aerial manipulator can be significantly expanded and out of the range of the airflow.

During most of the capture task process, the manipulator remains in the standby state. Therefore, the COM of the manipulator can be used to calculate the placement position of the battery by

$$m_m x_m^s = m_b x_b, \tag{1}$$

where x_m^s is the distance from the COM of the quadrotor UAV to the COM of the manipulator in standby state along x axis, x_b is the distance from the COM of the quadrotor UAV to the placement position of the battery along x axis.

B. Architecture and Components of the System

The proposed system (shown in Fig. 2) mainly consists of the aerial manipulator, the motion capture system (OptiTrack), and the ground station. The aerial manipulator is composed by a quadrotor UAV as the platform and a 5-DOF robotic arm with revolute joints and a gripper as the manipulator. The controller of the aerial manipulator runs on a STM32F7 microprogrammed control unit (MCU), which controls the quadrotor UAV and the manipulator at the same time. With respect to the actuator power unit, the motor type of the quadrotor UAV is Sunnysky Eolo 3510. The propeller

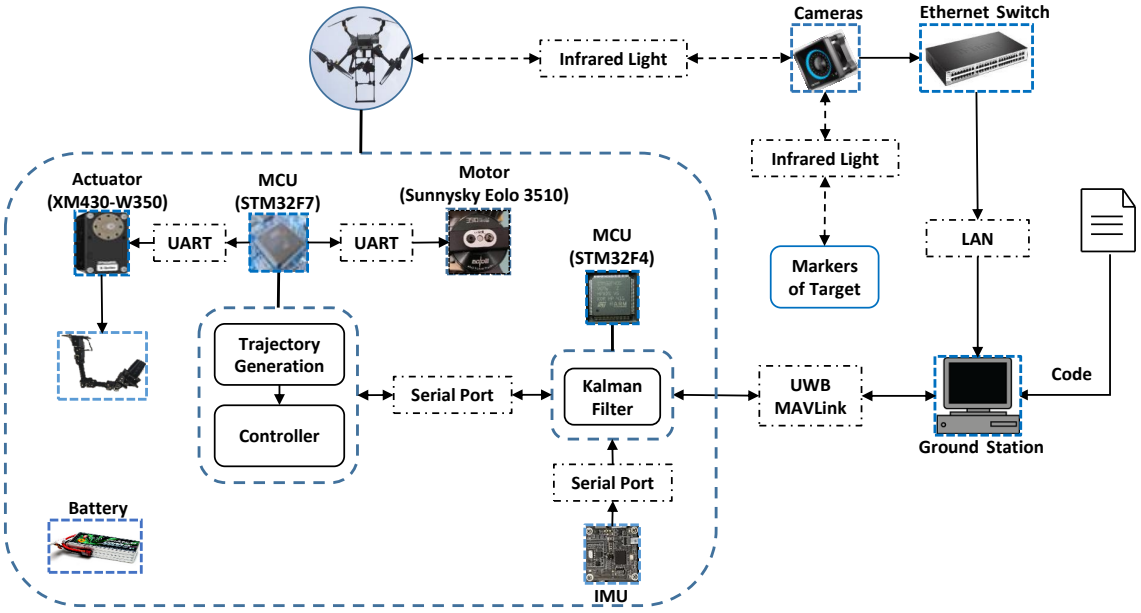

Fig. 3: System architecture.

radius and the propeller pitch are 19.05 cm and 12.7 cm respectively. The joints of the manipulator are driven by DYNAMIXEL XM-430 servo actuator with a stall torque of 4.1 N·m. The power is provided by a 6 cells Li-Po battery. With these configurations, the aerial manipulator has a maximum flight time of 20 min with a weight of 3.6 kg and a maximum payload capacity of 0.4 kg.

The OptiTrack system is a real-time tracking system with millimeter-level positioning accuracy which is used for low-latency, accurate 6-DOF tracking for rigid body. It has 10 Prime 22 cameras that can send out pulsed infrared light using the infrared LEDs. The infrared light can be reflected by markers attached on the target rigid body. Subsequently, the live video of the cameras is streamed over Ethernet to the ground station running software of Motive. The precision 6-DOF tracking of the rigid body can be calculated using triangulation with knowing the position of those markers in perspective of several cameras. The rigid body movement information including position and attitude can be captured when at least three markers are visible. In the aerial manipulator system, the OptiTrack system is used to track the movement information of the quadrotor UAV and the capture target in real time. In order to further improve the navigation accuracy, an inertial measurement unit (IMU) is adopted and a Kalman filter running on another STM32F4 MCU is used to fuse the attitude data of quadrotor UAV from IMU and OptiTrack.

The architecture of the aerial manipulator system is developed in Fig. 3. Once the movement information of the aerial manipulator and the target is obtained by OptiTrack system, the information is sent to the ground station over Ethernet subsequently. After the STM32F4 receives the message from the ground station over ultra wide band (UWB) network and the MAVLink protocol with the frequency of 400Hz, the data can be fused with information from IMU. The fused data is used to plan the trajectory online and generate control law in the STM32F7 running on 1000 Hz. Finally, the control signal is sent to the motor and servo actuator over UART serial port. The detailed implementation of trajectory generation and control will be described in Section III.

III. IMPLEMENTATION OF TRAJECTORY GENERATION AND CONTROL

A. Online Trajectory Generation Unit

Inspired by the predation maneuver of birds, an online trajectory generation law is proposed in this Section. Birds always face the food when hunting during flight. Therefore, it also makes sense to keep the aerial manipulator pointing towards its target at all times by adjusting the yaw angle of the quadrotor UAV. Based on this mechanism, the online trajectory generation law is designed according to the measured target position. During tracking process, if the position of the target changes, the trajectory and the yaw angle can be regenerated. To be more specific, the capture mission is divided into five steps:

- **Aim**: The yaw angle of the quadrotor UAV is changed so that the initial direction of the manipulator is pointed at the target. The target vector is defined in the North-East-Down (NED) coordinate as $\boldsymbol{d} = [d_x, d_y, d_z]^\top = \boldsymbol{p}_{tar} - \boldsymbol{p}$, where $\boldsymbol{p}_{tar}$ is the position of target. The

desired yaw angle can be obtained as

$$\psi_{des}=\begin{cases}\arctan\dfrac{d_y}{d_x}, & \text{if } d_x>0,\\ \arctan\dfrac{d_y}{d_x}+\pi, & \text{if } d_x<0 \text{ and } d_y\geq 0,\\ \arctan\dfrac{d_y}{d_x}-\pi, & \text{if } d_x<0 \text{ and } d_y<0,\\ \dfrac{\pi}{2}, & \text{if } d_x=0 \text{ and } d_y>0,\\ -\dfrac{\pi}{2}, & \text{if } d_x=0 \text{ and } d_y<0,\\ 0, & \text{if } d_x=0 \text{ and } d_y=0.\end{cases} \tag{2}$$

In order to keep the rotation smooth, the rotation speed of yaw angle is set to 0.785 rad/s in the experiment.

- **Approach**: The quadrotor UAV approaches the target with a certain speed and hovers at a fixed distance from the target. The trajectory generation law can be expressed as

$$\boldsymbol{p}_{sp}(t+dt)=\boldsymbol{p}_{sp}(t)+v_{sp}\frac{\boldsymbol{d}}{||\boldsymbol{d}||}, \tag{3}$$

where the v_{sp} is the set speed of approach. During aim and approach, the manipulator remains in the standby state. In the experiment, the joint angles are set as $[\pi,\pi,4.59,1.54,2.79]$ rad.
- **Manipulator Unfold**: The manipulator adjusts to the unfolding state and holds, waiting for the quadrotor UAV to get closer to the target. The joint angles are set to $[\pi,\pi,\pi,\pi,2.79]$ rad in the experiment.
- **Capture**: The quadrotor UAV further adjusts its position, and the manipulator clamps its gripper in the right position. The joint angle of the gripper is changed to 0.61 rad in practice.
- **Homeward Voyage**: The manipulator clamps the target and returns to the standby state. The quadrotor UAV flies back to the origin. The trajectory generation law is same as (3). The target point $\boldsymbol{p}_{tar}$ is changed to $[0,0,-1.5]$ m.

B. UAV Control Unit

1) Mathematical model of the quadrotor UAV: In this Section, Euler angles are used to describe the attitude of quadrotor UAV. Two coordinate systems are defined to build the mathematical model, namely, body-fixed frame B and world-fixed frame E. The former is fixedly connected with the quadrotor UAV and its origin is located at the COM of the quadrotor UAV. The latter is fixedly connected to the earth and its origin is located at the initial position of the aerial manipulator. The rotation matrix from B to E can be obtained as

$$\boldsymbol{R}=\begin{bmatrix}c_\psi c_\theta & -s_\psi c_\phi+c_\psi s_\theta s_\phi & s_\psi s_\phi+c_\psi s_\theta c_\phi\\ s_\psi c_\theta & c_\psi c_\phi+s_\psi s_\theta s_\phi & -c_\psi s_\phi+s_\psi s_\theta c_\phi\\ -s_\theta & c_\theta s_\phi & c_\theta c_\phi\end{bmatrix}. \tag{4}$$

The relationship between the angular velocity of the quadrotor UAV in B and Euler angles rate can be presented as

$$[p,q,r]^\top=\boldsymbol{T}(\eta)[\dot\phi,\dot\theta,\dot\psi]^\top, \tag{5}$$

where the mapping matrix $\boldsymbol{T}(\eta)$ can be presented as

$$\boldsymbol{T}(\eta)=\begin{bmatrix}1 & 0 & -s_\theta\\ 0 & c_\phi & s_\phi c_\theta\\ 0 & -s_\theta & c_\theta c_\phi\end{bmatrix}.$$

The quadrotor UAV dynamics can be represented based on Newton-Euler method as

$$\begin{bmatrix}m_s\boldsymbol{I}_{3\times3} & 0_{3\times3}\\ 0_{3\times3} & \boldsymbol{I}\end{bmatrix}\begin{bmatrix}\dot{\boldsymbol{v}}^E\\ \dot{\boldsymbol{\omega}}^B\end{bmatrix}+\begin{bmatrix}\boldsymbol{0}_{3\times1}\\ \boldsymbol{\omega}^B\times(\boldsymbol{I}\boldsymbol{\omega}^B)\end{bmatrix}=\begin{bmatrix}\boldsymbol{F}^E+\boldsymbol{G}^E\\ \boldsymbol{\tau}^B\end{bmatrix}. \tag{6}$$

To simplify the control law design, the thrust force and torques serve as control inputs. For the quadrotor UAV with "X" configuration, the relation between the thrust force generated by each motors and control inputs can be represented as

$$\begin{bmatrix}f\\ \tau_x\\ \tau_y\\ \tau_z\end{bmatrix}=\begin{bmatrix}1 & 1 & 1 & 1\\ -d_\phi & -d_\phi & d_\phi & d_\phi\\ d_\theta & -d_\theta & d_\theta & -d_\theta\\ c_\tau & -c_\tau & -c_\tau & c_\tau\end{bmatrix}\begin{bmatrix}f_1\\ f_2\\ f_3\\ f_4\end{bmatrix}. \tag{7}$$

2) Quadrotor UAV Controller Design:

- **Translational Controller**: Considering the desired trajectory $\boldsymbol{p}_d^E=[x_d,y_d,z_d]^\top$ and ψ_d, the control law of position loop is designed based on cascade PID theory as

$$\begin{cases}\boldsymbol{v}_d^E=\boldsymbol{K}_p(\boldsymbol{p}_d^E-\boldsymbol{p}^E)+\dot{\boldsymbol{p}}_d^E,\\ \boldsymbol{a}_d^E=\boldsymbol{K}_v(\boldsymbol{v}_d^E-\boldsymbol{v}^E)+\ddot{\boldsymbol{p}}_d^E+g\boldsymbol{e}_3,\\ \boldsymbol{F}_d^E=m_s\boldsymbol{a}_d^E,\end{cases} \tag{8}$$

where $\boldsymbol{K}_p$ and $\boldsymbol{K}_v$ are positive diagonal control gain matrices, $\boldsymbol{v}_d^E$ is a virtual control input, $\boldsymbol{e}_3=[0,0,1]^\top$ is a unit vector. The desired thrust forces can be obtained by projecting the desired force vector onto the z axis of B as

$$f=\boldsymbol{F}_d^E\cdot\boldsymbol{z}_b^E, \tag{9}$$

where $\boldsymbol{z}_b^E=\boldsymbol{R}\boldsymbol{e}_3$.
- **Differential Flatness Theory**: According to the idea of cascade control, the control input $\boldsymbol{F}_d^E$ needs to be achieved by the rotational controller. Therefore, it should be converted to the desired Euler angles $\boldsymbol{\eta}_d=[\phi_d,\theta_d,\psi_d]^\top$. In this paper, the differential flatness theory is used to solve the problem. The desired rotation matrix can be obtained as $\boldsymbol{R}_d=[\boldsymbol{x}_{b,d}^E,\boldsymbol{y}_{b,d}^E,\boldsymbol{z}_{b,d}^E]$. The desired z axis of body-fixed frame is defined as

$$\boldsymbol{z}_{b,d}^E=\frac{\boldsymbol{F}_d^E}{||\boldsymbol{F}_d^E||}. \tag{10}$$

The desired yaw angle is ψ_d. The x axis in the intermediate frame can be represented as $\boldsymbol{x}_{c,d}^E=[c_{\psi_d},s_{\psi_d},0]^T$. The $\boldsymbol{y}_{b,d}^E$ and $\boldsymbol{x}_{b,d}^E$ are driven as follows

$$\boldsymbol{y}_{b,d}^E=\frac{\boldsymbol{z}_{b,d}^E\times\boldsymbol{x}_{c,d}^E}{\left|\left|\boldsymbol{z}_{b,d}^E\times\boldsymbol{x}_{c,d}^E\right|\right|},\quad \boldsymbol{x}_{b,d}^E=\boldsymbol{y}_{b,d}^E\times\boldsymbol{z}_{b,d}^E. \tag{11}$$

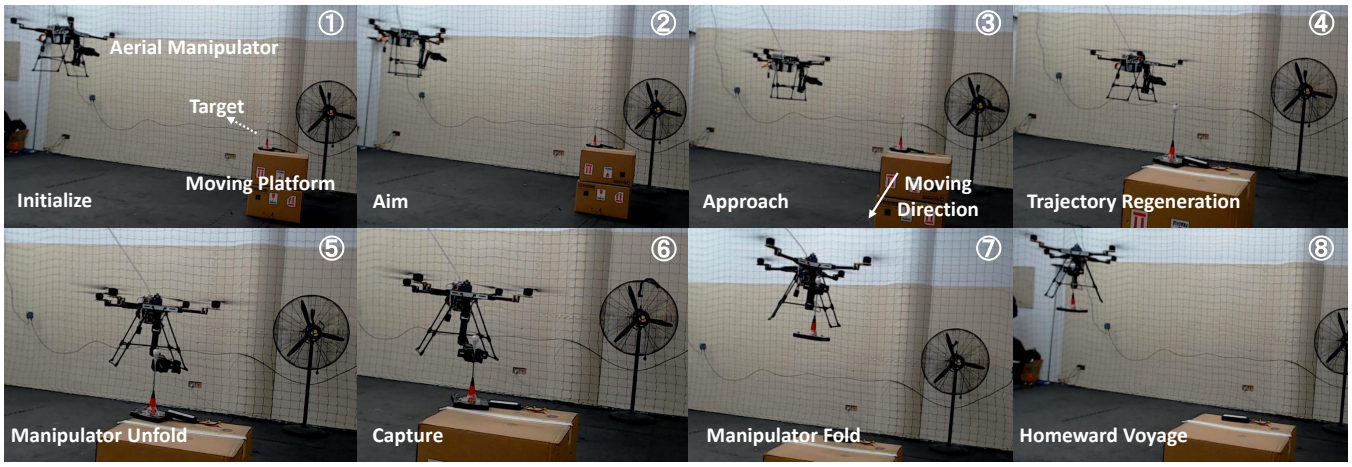

Fig. 4: Experiment scenario. The aerial manipulator generates its trajectory in real time according to the position of the target and achieves the capture mission. Flight video is available in https://youtu.be/HLBBCmGPNA4.

Combined with (4), the desired Euler angles can be obtained as $\phi_d = \arctan(r_{32}/r_{33})$, $\theta_d = -\arcsin(r_{31})$, where the r stands for the element of $\boldsymbol{R}_d$.

- **Rotational Controller**: The basic idea of the rotational controller is cascade PID and feedback linearization. First, a virtual control over the Euler angles rate can be formulated as

$$\dot{\boldsymbol{\eta}}_r = \boldsymbol{K}_\eta(\boldsymbol{\eta}_d - \boldsymbol{\eta}) + \dot{\boldsymbol{\eta}}_d. \tag{12}$$

Combined with (5), the desired angular speed in B can be defined as follows

$$\boldsymbol{\omega}_d = T(\boldsymbol{\eta})\dot{\boldsymbol{\eta}}_r. \tag{13}$$

Next, in a similar way, consider the angular speed tracking error $\boldsymbol{e}_\omega = \boldsymbol{\omega}_d - \boldsymbol{\omega}$, another virtual control over the angular acceleration can be formulated as

$$\boldsymbol{\zeta}_d = \boldsymbol{K}_{P\omega}\boldsymbol{e}_\omega + \boldsymbol{K}_{D\omega}\dot{\boldsymbol{e}}_\omega + \boldsymbol{K}_{I\omega}\int_0^t \boldsymbol{e}_\omega \mathrm{d}t + \dot{\boldsymbol{\omega}}_\mathrm{d}. \tag{14}$$

Combined with (6), the control torque input can be calculated as

$$\boldsymbol{\tau}^B = \boldsymbol{I}\boldsymbol{\zeta}_d + \boldsymbol{\omega}^B \times (\boldsymbol{I}\boldsymbol{\omega}^B). \tag{15}$$

In the above formulas, $\boldsymbol{K}_\eta$, $\boldsymbol{K}_{P\omega}$, $\boldsymbol{K}_{D\omega}$, and $\boldsymbol{K}_{I\omega}$ are positive diagonal control gain matrices. In fact, the controller compensates all nonlinear terms of the quadrotor UAV. The control gain matrices can be viewed as control gains for the first order integrator and easy to be designed.

C. Manipulator Control Unit

The controller of the manipulator in this paper is in joint angle mode, which implies that the manipulator can track the reference joint angles smoothly. D-H parameters are used to describe the structure of the manipulator as shown in Table. II. These parameters can be used to precisely calculate the position and orientation of the gripper relative to B by using the forward kinematics.

TABLE II: Physical Parameters of the Manipulator

	d(mm)	θ(°)	a(mm)	α(°)
Link1	59.5	-180	0	-90
Link2	0	100	130.2	0
Link3	0	80	124	0
Link4	0	0	126	90
Gripper	0	0	81.7	0

IV. EXPERIMENT RESULT

A. Scenario

As shown in Fig. 4, the aerial manipulator is assigned a capture mission. The target is set on a moving platform. During approaching process, the platform moves from its original position to another point. Therefore, the aerial manipulator needs to regenerate its trajectory in real time.

B. Results and Analysis

As the platform moves, the aerial manipulator can track the target in real time (see Fig. 5). When the platform stops at the final point, the aerial manipulator begins to execute the grasping actions including manipulator unfold and capture. After reaching the designated point, the manipulator adjusts to the unfolding state and holds. The quadrotor UAV further adjusts its position closer to the target so that the gripper of the manipulator can grip the target.

Fig. 6 shows that the aerial manipulator begins regenerating its trajectory about 4 s. The desired yaw angle changes firstly. About 20 s, the aerial manipulator tunes its position in the x and y direction. Also about 20 s, the gripper of the manipulator (joint 5) changes to 0.61 rad, which implies gripper closing, as shown in Fig. 7.

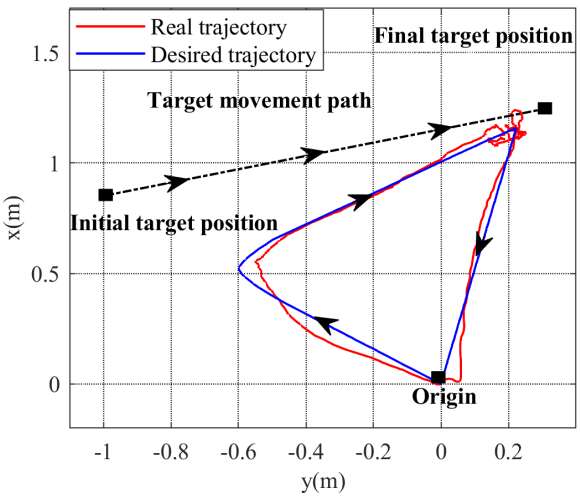

Fig. 5: The trajectory of the aerial manipulator in $x-y$ plane during the capture mission.

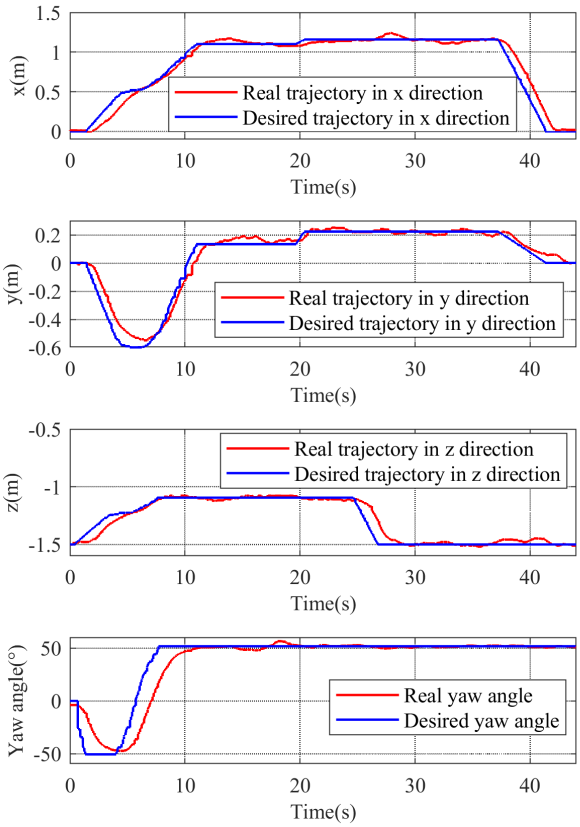

Fig. 6: The trajectory and yaw angle of the aerial manipulator during the capture mission.

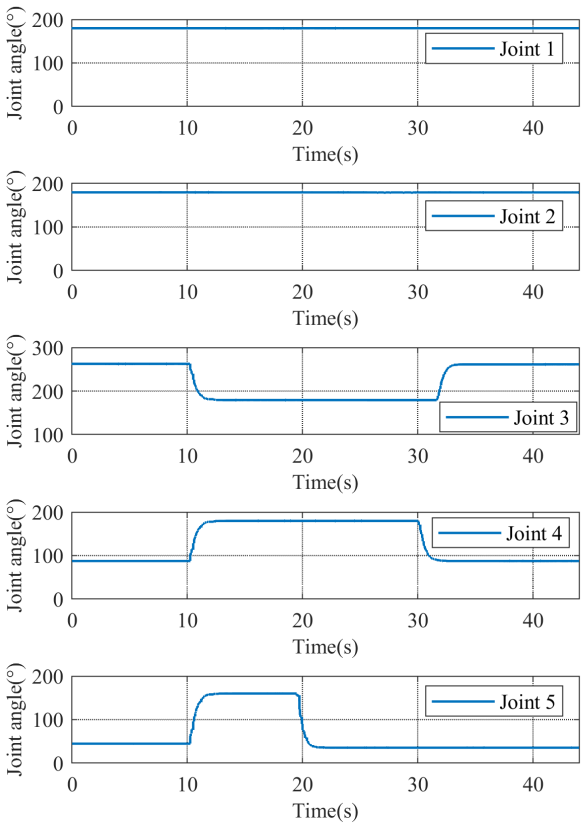

Fig. 7: The joint angles of the manipulator during during the capture mission.

During the capture mission, the mean absolute position error of the quadrotor UAV is 0.08 m. However, during the grasping actions including manipulator unfold and capture (11-37 s), the mean absolute position error is only 0.05 m. Moreover, the manipulator can track the reference joint angles smoothly during the whole mission as shown in Fig. 7. As a result, the target is captured successfully.

V. CONCLUSIONS

In this paper, an aerial manipulator system with novel mechanical layout is designed and applied to capture a moving target. The benefits of this system include: (1) The task space of aerial manipulator is expended and out of the range of the airflow generated by the quadrotor UAV. (2) The proposed online trajectory generation module can generate an effective trajectory for capture missions in real time. These improvements offer the potential for the aerial manipulator adapting to more complicated tasks.

REFERENCES

[1] K.X. Guo, J.D. Jia, X. Yu, L. Guo, and L.H. Xie, "Multiple observers based anti-disturbance control for a quadrotor UAV against payload and wind disturbances," Control Engineering Practice, vol. 102, pp. 104560, 2020.

[2] X. Meng, Y. He, and J. Han, "Survey on aerial manipulator: system, modeling, and control," Robotica, vol. 38, no. 7, pp. 1288-1317, 2020.

[3] X. L. Ding, P. Guo, K. Xu, and Y. S. Yu, "A review of aerial manipulation of small-scale rotorcraft unmanned robotic systems," Chinese Journal of Aeronautics, vol. 32, no. 1, pp. 200-214, 2019.

[4] F. Ruggiero, V. Lippiello and A. Ollero, "Aerial manipulation: a literature review," IEEE Robotics and Automation Letters, vol. 3, no. 3, pp. 1957-1964, July 2018.

[5] G. Heredia, A.E. Jimenez-Cano, I. Sanchez, D. Llorente, V. Vega, J. Braga, J. A. Acosta, and A. Ollero, "Control of a multirotor outdoor aerial manipulator," 2014 IEEE/RSJ International Conference on Intelligent Robots and Systems, Chicago, IL, USA, pp. 3417-3422, 2014.

[6] M. J. Kim, K. Kondak and C. Ott, "A stabilizing controller for regulation of UAV with manipulator," IEEE Robotics and Automation Letters, vol. 3, no. 3, pp. 1719-1726, July 2018.

[7] J. Thomas, J. Polin, K. Sreenath, V. Kumar, "Avian-inspired grasping for quadrotor micro UAVs." ASME 2013 international design engineering technical conferences and computers and information in engineering conference, American Society of Mechanical Engineers Digital Collection, 2013.

[8] K. Kondak, F. Huber, M. Schwarzbach, M. Laiacker, D. Sommer, M. Bejar, and A. Ollero, "Aerial manipulation robot composed of an autonomous helicopter and a 7 degrees of freedom industrial manipulator," 2014 IEEE International Conference on Robotics and Automation (ICRA), Hong Kong, China, pp. 2107-2112, 2014.

[9] G. Zhang, Y. He, B. Dai, F. Gu, J. Han and G. Liu, "Robust control of an aerial manipulator based on a variable inertia parameters model," IEEE Transactions on Industrial Electronics, vol. 67, no. 11, pp. 9515-9525, Nov 2020.

[10] V. Lippiello and F. Ruggiero, "Exploiting redundancy in Cartesian impedance control of UAVs equipped with a robotic arm," 2012 IEEE/RSJ International Conference on Intelligent Robots and Systems, Vilamoura-Algarve, Portugal, pp. 3768-3773, 2012.

[11] V. Lippiello, and F. Ruggiero. "Cartesian impedance control of a UAV with a robotic arm." IFAC Proceedings vol. 45, no. 22, pp. 704-709, 2012.

[12] F. Ruggiero, M.A. Trujillo, R. Cano, H. Asorbe, A. Viguria, C. Perez, V. Lippiello, A. Ollero, and B. Siciliano, "A multilayer control for multirotor UAVs equipped with a servo robot arm," 2015 IEEE International Conference on Robotics and Automation (ICRA), Seattle, WA, USA, pp. 4014-4020, 2015.

[13] N. Staub, D. Bicego, Q. Sabl, V. Arellano, S. Mishra and A. Franchi, "Towards a flying assistant paradigm: the OTHex," 2018 IEEE International Conference on Robotics and Automation (ICRA), Brisbane, QLD, Australia, pp. 6997-7002, 2018.

[14] M. Kobilarov. "Nonlinear trajectory control of multi-body aerial manipulators." Journal of Intelligent & Robotic Systems, vol. 73, no.1, pp. 679-692, 2014.

[15] H. Yang and D. Lee, "Dynamics and control of quadrotor with robotic manipulator," 2014 IEEE International Conference on Robotics and Automation (ICRA), Hong Kong, China, pp. 5544-5549, 2014.

[16] M. Fanni and A. Khalifa, "A new 6-DOF quadrotor manipulation system: design, kinematics, dynamics, and control," in IEEE/ASME Transactions on Mechatronics, vol. 22, no. 3, pp. 1315-1326, June 2017.

[17] S. Kannan, A.O. Miguel, and V. Holger. "Modeling and control of aerial manipulation vehicle with visual sensor," IFAC Proceedings, vol. 46, no. 30, pp. 303-309, 2013.

[18] H. Zhong et al., "A practical visual servo control for aerial manipulation using a spherical projection model," IEEE Transactions on Industrial Electronics, vol. 67, no. 12, pp. 10564-10574, Dec. 2020.